

PAPER • OPEN ACCESS

Utilizing numerical models to identify process-induced residual stresses in 3D woven carbon/epoxy composites

To cite this article: Igor Tsukrov *et al* 2018 *IOP Conf. Ser.: Mater. Sci. Eng.* **406** 012030

View the [article online](#) for updates and enhancements.



IOP | **ebooks**TM

Bringing you innovative digital publishing with leading voices to create your essential collection of books in STEM research.

Start exploring the collection - download the first chapter of every title for free.

Utilizing numerical models to identify process-induced residual stresses in 3D woven carbon/epoxy composites

Igor Tsukrov^{1,*}, Kostiantyn Vasylevskyi¹, Borys Drach², Hilary Buntrock¹, Todd Gross¹

¹University of New Hampshire, Durham, NH 03861, USA

²New Mexico State University, Las Cruses, NM 88003, USA

* igor.tsukrov@unh.edu

Abstract. A combined experimental-numerical procedure is proposed to evaluate residual stresses in 3D woven carbon/epoxy composites. It is assumed that residual stresses are caused by the difference in thermal expansion coefficients of the constituents. The impact of residual stresses is quantified by drilling blind holes in the composite panels and mapping the resulting in-plane surface displacements by digital image correlation and electronic speckle pattern interferometry. Then mesoscale finite element models of the composite are used to determine the effective temperature drop ΔT^{eff} that results in the same predictions for hole drilling. The local distributions of residual stress are given by the finite element simulations of the cooling by this temperature drop ΔT^{eff} .

1. Introduction

3D woven carbon/epoxy composites develop curing-induced residual stresses that might limit their performance or lead to microcracking [1]. Distribution of the process-induced stresses can be quite complex due to morphology of the reinforcement and various residual stress formation mechanisms, e.g. inhomogeneity of the resin flow and temperature during injection and cure, chemical shrinkage, and mismatch between fiber and resin coefficients of thermal expansion (CTEs). There are no direct experimental techniques to determine this distribution. However, mesoscale numerical models of woven composites have been proven to provide a meaningful insight into the mechanics of the textile composites [2].

In this paper, we investigate whether recently developed finite element (FEA) models [3] can be utilized to determine the spatial variation of process-induced residual stresses from the surface displacements observed after drilling a hole. The surface displacements are measured by digital image correlation (DIC) and electronic speckle pattern interferometry (ESPI). The two methods are used because the displacements are sometimes on the lower end of the resolution for the DIC method and the displacement gradients near the hole are sometimes too steep to resolve the fringes obtained via the ESPI method.

There have been previous publication utilizing FEA or analytical solutions to evaluate residual stresses in the composites based on the hole drilling technique and interpretation of ESPI measurements, see [4, 5]. However, in those studies it was assumed that the residual stresses were uniform in the volume occupied by the hole which is not accurate for 3D woven composites. In our research, we assume that local distribution of residual stresses arises during cooling after curing and is mostly caused by the difference in CTEs between the fibers and the matrix. Thus, in our approach we compare the displacements from hole drilling with the results of FEA simulations to determine such an effective temperature drop ΔT^{eff} that the resulting distribution of stresses causes the same surface displacements. We then assume that the stress distribution caused by ΔT^{eff} is the actual residual stress field.



Content from this work may be used under the terms of the [Creative Commons Attribution 3.0 licence](#). Any further distribution of this work must maintain attribution to the author(s) and the title of the work, journal citation and DOI.

2. Experimental Methods

Experimental measurements were conducted on 4.1 mm thick composite panels fabricated by Albany Engineered Composites using Hexcel RTM6 resin and Hexcel 12K IM7 PAN-based carbon fibers. Several reinforcement architectures with different level of through-thickness reinforcement were considered but this paper presents results for only one of them, the so-called one-by-one orthogonal. This particular architecture was chosen because of its high through-thickness constraint preventing in-plane residual stress relaxation mechanism typical for laminates and low through-thickness constraint composites. The material had an overall fiber volume fraction of 55%. The in-plane dimensions of the repeating unit (as shown in figure 1) were 5.1 mm by 5.1 mm.

The composite sections containing at least nine unit cells were cut out from the panels and painted first with white, high heat spray paint. The black speckles were applied using an airbrush to get speckles that ranged in size from 5 to 10 μm . Then the surface was covered with a clear matte spray paint to protect the speckles from drilling debris deposits and prevent the speckles being removed with the water used for cooling during drilling. The sample was glued on a block mounted on a Thor Labs kinematic mount to allow precise repositioning of the “before drilling” and “after drilling” DIC images and interferograms. The apparent placement repeatability was on the order of 5 μm or less. The same specimen was probed on both the DIC setup and the interferometry system.

Residual stresses were studied by drilling a 1mm diameter blind hole to a depth of 0.5 mm and recording the resulting in-plane displacements on the surface of the specimen. Drilling was done with UKAM diamond coring tool. The depth was continuously measured with a dial indicator attached to the drilling head. A continuous flow of deionized water was manually applied during drilling using a squeeze bottle. The water was used to minimize the heat generated during drilling and to carry away the drilling debris. The sample was rinsed with more water after drilling and dried with a flow of warm air.

The in-plane displacements in the near field region around the hole were determined with a VIC-Micro3D Correlated Solutions digital image correlation system. The pixel size was 3.34 μm . The typical quoted maximum resolution is 0.01 pixels. The apparent displacement noise is ~ 0.05 pixels which corresponds to $\sim 0.06 \mu\text{m}$. The sampled region was large enough so that we subtracted any tilt and displacement from replacing the sample by performing a 2D first order, least squares fit of a 10-pixel wide region on the outer border of the image. When the apparent displacement field extended to the border, the tilt correction was only performed on the borders not impacted by the displacement field of the hole.

The displacements outside the high displacement gradient region around the hole were measured using a custom-built electronic speckle pattern interferometry system similar to the one described by Diaz et al [6]. We used a 50 mW Melles Griot HeNe laser that had linear polarization. The angle between the normal to the specimen and the illumination beams was 45° which resulted in a 448 nm displacement for a phase difference corresponding to 2π . Our system exhibited phase noise of $<\pi/25$ which corresponds to a displacement of 9 nm which is roughly 7 times lower than the DIC measurements.

3. FEA modeling

This research utilized meso-scale FEA models of 3D woven composites described in publications [3, 7]. They were developed for the smallest repeating portion of the material – the so-called “unit cell” (UC). The entire composite can then be considered as a continuous assemblage of such unit cells. For this study we used the numerically simulated geometry of woven reinforcement obtained with Dynamic Fabric Mechanical Analyzer (DFMA), see [8]. Figure 1 presents an example of 3D finite element model for the orthogonally reinforced composite developed in MSC Marc Mentat [9].



Figure 1. Unit cell of one-by-one orthogonal composite panel: from the initial schematics of the reinforcement for DFMA simulations to the finite element mesh (reinforcement + matrix) in MSC Marc Mentat.

The matrix (fully cured HEXCEL RTM6 epoxy resin) was simulated as a linear isotropic material with constant Poisson's ratio $\nu_m = 0.35$, and temperature dependent Young's modulus E_m and thermal expansion coefficient α_m :

$$E_m = E_m^{0^\circ\text{C}} - \beta_m T \quad (1)$$

$$\alpha_m = \alpha_m^{0^\circ\text{C}} + \gamma_m T \quad (2)$$

where $E_m^{0^\circ\text{C}} = 3,500 \text{ MPa}$, $\beta_m = 5.9 \frac{\text{MPa}}{\text{^\circ C}}$, $\alpha_m^{0^\circ\text{C}} = 5 \cdot 10^{-5} \frac{1}{\text{K}}$, $\gamma_m = 1.05 \cdot 10^{-7} \frac{1}{\text{K} \cdot \text{^\circ C}}$ are the material parameters, and T is the temperature in $^\circ\text{C}$. The tows (12,000 IM7 carbon fibers impregnated with RTM6 epoxy) were simulated as transversely isotropic material with the properties obtained by micromechanical modeling as $E_{1t} = 221.38 \text{ GPa}$, $E_{2t} = 13.18 \text{ GPa}$, $G_{12t} = 7.17 \text{ GPa}$, $\nu_{12t} = 0.35$, $\nu_{23t} = 0.35$, $\alpha_{1t} = -2.29 \cdot 10^{-7} \frac{1}{\text{K}}$, $\alpha_{2t} = 2.23 \cdot 10^{-5} \frac{1}{\text{K}}$. In these expressions, direction 1 is parallel to the axis of the tow and directions 2 and 3 are transverse to the tow axis. Note that even though the properties of the matrix in the tows change with temperature as given by formulas (1) and (2), these changes will result in insignificant variations of the homogenized properties of the tows (see comparison in [7]), so in the numerical simulations the properties of the tows were assumed to be temperature independent.

The hole drilling was simulated in MSC Marc Mentat by deactivating elements belonging to the hole. First, the simulation of the cooling by the equivalent temperature drop ΔT^{eff} was performed. Then the elements corresponding to the position of the hole were manually selected to deactivate. Subtracting the displacements obtained after the simulation of curing from the displacements caused by removing the elements representing the hole produces the displacement field from the hole drilling.

In the simulations, upper and lower surfaces of UC were not constrained because the cell includes the entire thickness of the composite panel. Selection of the lateral constraints for hole drilling modeling, however, presented certain challenges. Periodic boundary conditions, traditionally used to evaluate the overall performance of woven composites, are not appropriate when the hole is located close to the boundary of the unit cell. For example, consider distribution of displacements due to hole drilling predicted by FEA for 2 different hole locations, see figure 2. Analysis of the lower right image shows that FEA predicts some unrealistically increased displacements far from the hole due to the imposed symmetry condition. On the other hand, FEA modelling of the entire composite panel with the same level of accuracy would require extremely large finite element models and excessive requirements for computer time and resources.

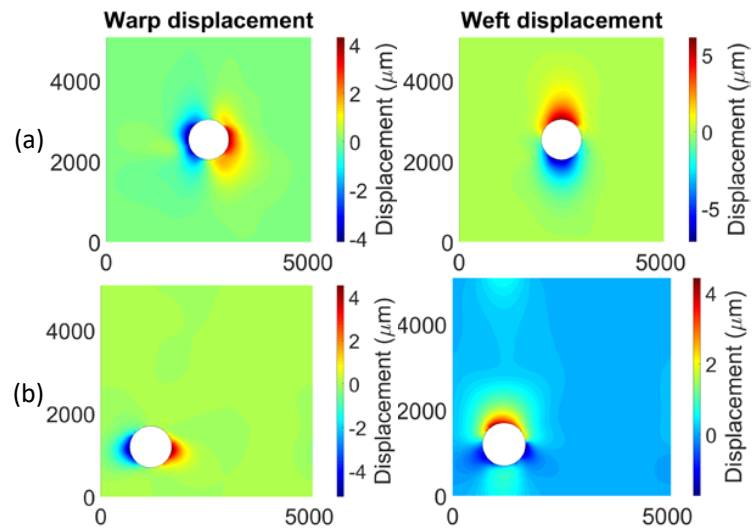


Figure 2. FEA-predicted displacement fields due to the temperature drop and subsequent removal of the elements simulating hole drilling: (a) displacements for centrally located hole; (b) displacements for hole near the corner of UC.

To select the most efficient way to model the structure we considered 3 possible approaches to selecting lateral boundary conditions. The most accurate one considered a portion of the structure consisting of 9 unit cells (3×3) with the sides that are required to be periodic but are allowed to move laterally to accommodate the overall shrinkage of the composite panel due to cooling. In the second approach, one unit cell is surrounded by the equivalent effective material and the periodicity is not imposed. In this case the required number of finite elements and, correspondingly, the simulation time was significantly lower. And, finally, the third approach was to consider one unit cell without the periodicity conditions. We calculated the displacements of the material due to cooling and normalized them with respect to 3×3 results, which we consider to be the most accurate. Based on the comparison presented in figure 3, we decided to perform our hole drilling simulations utilizing the model of a unit cell surrounded by the equivalent material (second approach).

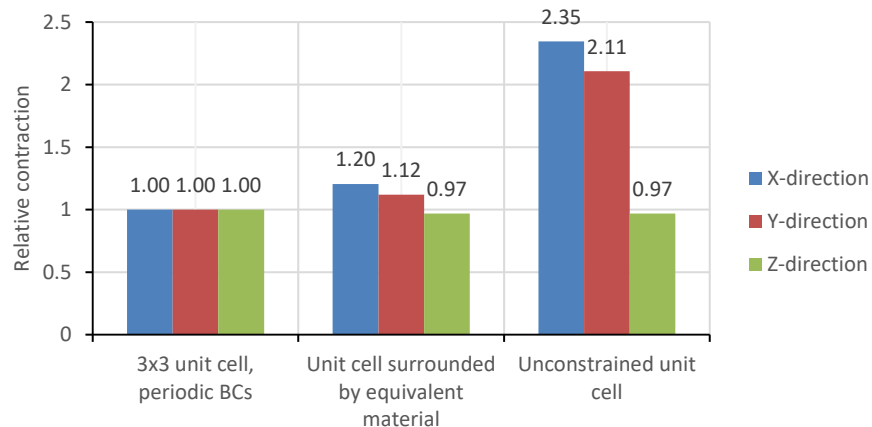


Figure 3. Comparison of predicted displacements in warp (x), weft (y), and through-thickness (z) directions for three choices of lateral boundary conditions (normalized with respect to 3×3 results).

4. Results and discussion

Our method is illustrated for the experimental measurements performed for a hole located as shown in figure 4. As can be deduced from the DIC images depicted in figure 5(b), the material removed by the hole was

mostly in the state of in-plane tension, so drilling resulted in opening of the hole. To determine the effective temperature drop ΔT^{eff} , we used the approach similar to that implemented in [4]. We matched FEA predictions for warp and weft displacements at the points located at a prescribed distance from the hole (in our case, we selected points one diameter away from the hole edge) with the experimental measurements. This resulted in the effective temperature drop $\Delta T^{\text{eff}} = -35^{\circ}\text{C}$. Figure 5(a) shows distributions of weft and warp displacements predicted by FEA for this temperature drop. Figure 5(c) presents displacements along the lines shown in figure 5(b), both experimentally observed and numerically predicted. Overall, good correspondence is observed with the exception of the weft displacements to the left of the lower left image, which was the area of significant decorrelation in experimental measurements.

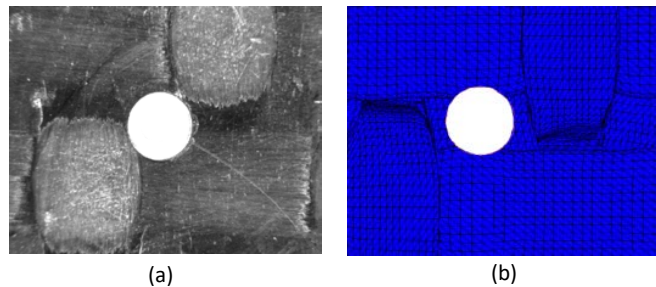


Figure 4. Microscope image of the drilled hole vs. FE model with matrix elements not shown.

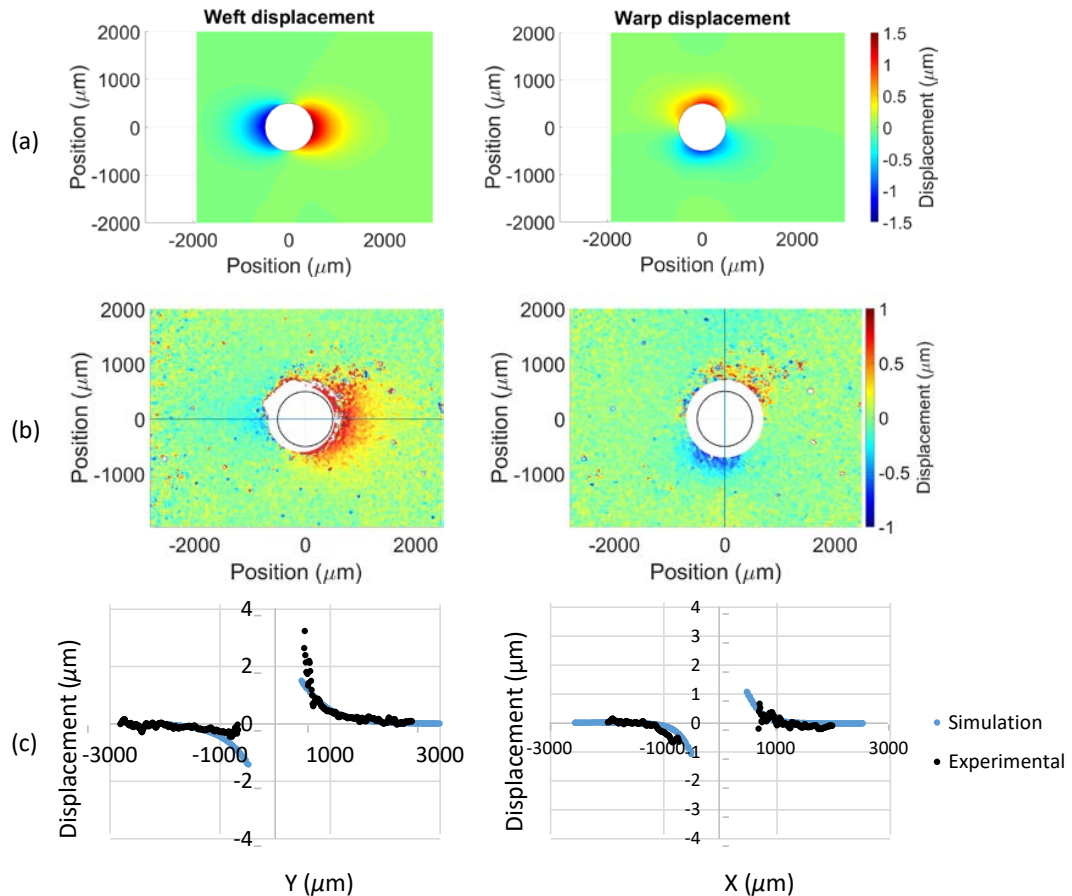


Figure 5. Displacement fields caused by hole drilling: (a) FEA predictions; (b) experimental DIC measurements; (c) slice plots along the lines shown in (b).

After the effective temperature drop ΔT^{eff} is determined and validated by comparison with the DIC and ESPI data, FEA simulations can be used to evaluate distribution of cure-induced residual stresses due to mismatch in CTE of constituents. Figure 6 presents distribution of residual stresses in both warp and weft directions (σ_{XX} and σ_{YY}), as well as the hydrostatic and von-Mises stress. The hydrostatic stress is of particular interest as it plays a major role in development of matrix microcracking for 3D woven composites utilizing thermoset resins, as discussed, for example, in [7].

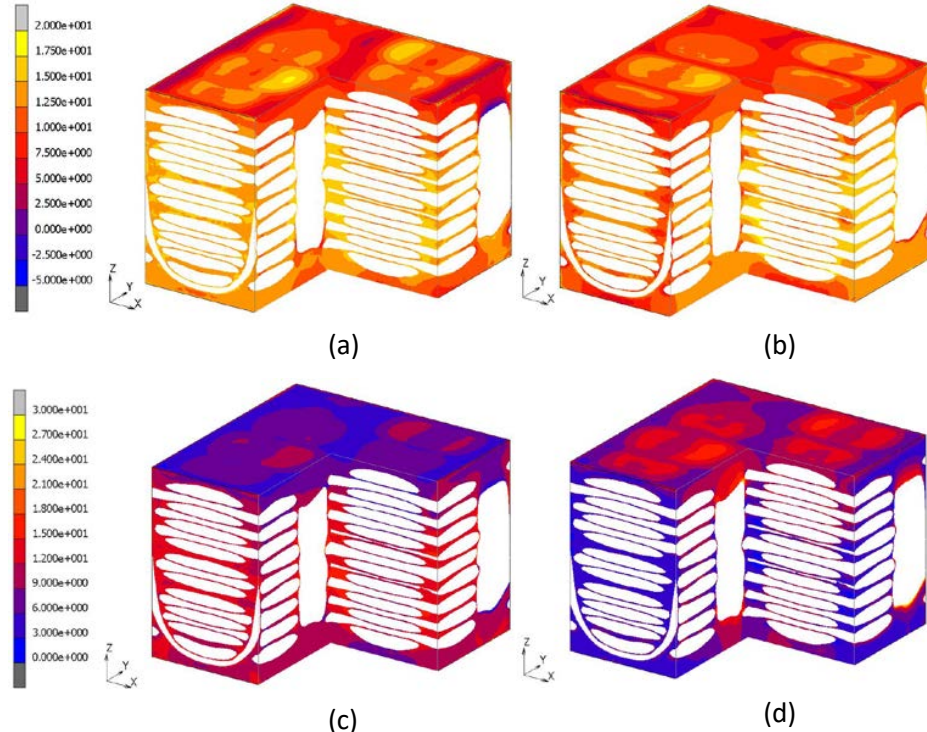


Figure 6. Distribution of cure-induced residual stresses in the matrix of orthogonally reinforced 3D woven composite: (a) warp; (b) weft; (c) hydrostatic; (d) equivalent von Mises.

5. Conclusions

Combination of meso-scale FEA modeling with experimental measurements of surface displacements caused by drilling blind holes in selected locations can be utilized to identify the full volume distribution of process-induced residual stresses in 3D woven composites. The proposed procedure involves determining the effective temperature drop ΔT^{eff} such that the surface displacements observed in the measurements are well reproduced by the numerical simulations of cooling by ΔT^{eff} and then removing the elements in the location of the drilled hole. In modelling, it is important to select the appropriate boundary conditions especially when the hole is drilled near the edge of the unit cell. The procedure can be used to evaluate levels of residual stresses in textile composites with various reinforcement architectures, and to optimize the material design by selecting the most beneficial reinforcement patterns and curing schedules.

Acknowledgements

This material is based upon work supported by the National Science Foundation through grant CMMI-1662098.

References

- [1] Tsukrov I, Bayraktar H, Giovinazzo M, Goering J, Gross T, Fruscello M and Martinsson L 2012 Finite element modeling to predict cure-induced microcracking in three-dimensional woven composites *Int. J. Fracture* **172** 209–16
- [2] Lomov S, Ivanov D, Verpoest I, Zako M, Kurashiki T, Nakai H and Hirosawa S 2007 Meso-FE modelling of textile composites: road map, data flow and algorithms *Compos. Sci. Technol.* **67** 1870–91
- [3] Drach A, Drach B and Tsukrov I 2014 Processing of fiber architecture data for finite element modeling of 3D woven composite *Adv. Eng. Softw.* **72** 18–27
- [4] Wu L F, Zhu J G and Xie H M 2015 Investigation of residual stress in 2D plane weave aramid fibre composite plates using Moiré interferometry and hole-drilling technique *Strain* **51** 429–43
- [5] Pisarev V S, Eleonsky S I, Chernov A V 2014 Residual stress characterization in orthotropic plate by combining hole-drilling method and speckle interferometry *29th Congress of the Int. Council of the Aeronautical Sciences* (St. Petersburg, Russia)
- [6] Diaz F V, Kaufmann G H and Galizzi G E 2000 Determination of residual stresses using hole drilling and digital speckle pattern interferometry with automated data analysis *Opt. Lasers Eng.* **33** 39–48
- [7] Drach B, Tsukrov I, Trofimov A, Gross T and Drach A 2018 Comparison of stress-based failure criteria for prediction of curing induced damage in 3D woven composites. *Compos. Struct.* **189** 366–77
- [8] Miao Y, Zhou E, Wang Y, and Cheeseman B 2008 Mechanics of textile composites: micro-geometry *Compos. Sci. Technol.* **68** 1671–8
- [9] <http://www.mscsoftware.com/product/marc>